Supporting Information

Redox Acceptor-Acceptor Nitro Functionalized Naphthalene diimide/rGO Anode for Sustainable Lithium-Ion Batteries

Madan R. Biradar,[a,b]† Nitish Kumar,[c,d]† Prakash Kumar Pathak,[c]† Sidhanath V. Bhosale,[a,b]* Sheshanath V. Bhosale,[e]* Rahul R. Salunkhe,[c]*

[a]Polymers and Functional Materials Division, CSIR-Indian Institute of Chemical Technology, Hyderabad-500007, Telangana, India.

[b]Academy of Scientific and Innovative Research (AcSIR), Ghaziabad- 201002, Uttar Pradesh, India.

[c]Materials Research Laboratory, Department of Physics, Indian Institute of Technology Jammu, Jagti, NH-44, PO Nagrota, Jammu, J&K, 181221, India.

[d]Department of Industrial and Materials Science, Chalmers University of Technology, Göteborg, SE-412 96 Sweden.

[e]Department of Chemistry, School of Chemical Sciences, Central University of Karnataka, Kalaburagi- 585 367, Karnataka, India.

*Corresponding Authors

bhosale@iict.res.in (Dr. Sidhanath V. Bhosale);
bsheshanath@gmail.com (Dr. Sheshanath V. Bhosale);
rahul.salunkhe@iitjammu.ac.in (Prof. Rahul R. Salunkhe).

†*These authors contributed equally to this work.*

NOTE S1

Materials.

1,4,5,8-Naphthalene tetracarboxylic dianhydride (NDA), 3,5-dinitroaniline (3,5-dNA) graphite powder, Sodium hydroxide (NaOH, 96%), Sodium nitrate ($NaNO_3$) Methanol anhydrous (MeOH, 99.5%), Ethanol anhydrous (EtOH, 99.5%) were purchased from Sigma-Aldrich (Bengaluru) Pvt. Ltd., India and Merck (Mumbai) Pvt. Ltd., India. 4-Nitroaniline (*p*NA) was purchased from AVRA India, hydrogen peroxide (H_2O_2, ≥ 30%) and potassium permanganate ($KMnO_4$) were purchased from Alfa Aesar Pvt. Ltd., India. Sulphuric acid (H_2SO_4), N, N – dimethyl formamide (DMF) and other solvents were purchased from Finar (Ahmadabad/Mumbai), Spectrochem (Mumbai) and Merck (Mumbai), India, and they were used without further purification unless otherwise stated. Deionized water was used throughout the whole experiment. Thin layer chromatography (TLC) (Merck Co.) was performed using 0.25 mm thick plates pre-coated with silica gel (40–60 mm, F254) and visualized using UV light (254 and 365 nm).

Synthesis of 2,7-bis(4-nitrophenyl)benzo[lmn][3,8]phenanthroline-1,3,6,8(2H,7H)-tetraone (NDI-2NO2).

A stirred solution of NDA (0.500 g, 1.864 mM) was added to a *p*-nitro aniline (*p*NA) (0.643 g, 4.66 mM) in 20 mL DMF. The resulting solution was stirred and refluxed for 12 h. The obtained mixture was allowed to cool to room temperature, and the crystalline solid was precipitated, which was washed with distilled water and dried under vacuum to afford the desired compound as an off-white solid. Yield 0.640 g (67.65%); [S1]

^{1}H NMR (DMSO-d_6 400 MHz) δ ppm = 8.76 (s, 4H), 8.47-8.44 (d, 4H), 7.83 – 7.81 (dd, 4H). ^{1}H NMR spectra were recorded on a Bruker Avance-400 MHz spectrometer at 300 °.
HR-MS (ESI) *m/z* calculated for $C_{26}H_{12}O_8N_4$: 508.06536; Found: $[M]^+$ 508.06496. HRMS was carried out on the Thermofisher Exactive Orbitrap instrument.

Synthesis of 2,7-bis(3,5-dinitrophenyl)benzo[lmn][3,8]phenanthroline-1,3,6,8(2H,7H)-tetraone (NDI-4NO$_2$)

The mixture of 1,4,5,8-naphthalene tetracarboxylic dianhydride (NDA) (0.500 g, 1.864 mM) and a 3,5-dinitroaniline (*3,5-d*NA) (0.8535 g, 4.66 mM) in 30 mL DMF was stirred for 5 min, and the resulting solution was reflux for 24 h. The obtained mixture was allowed to cool to room temperature and poured into cold water. The precipitate was collected and washed with water and methanol. The

residue was dried under a vacuum to make the desired compound an off-white solid. Yield 0.854 g (77.63%);

^{1}H NMR (DMSO-d_6 400 MHz) δ ppm = 9.01 (m, 2H), 8.96 (d, 4H), 8.82 (s, 4H).

HR-MS (ESI) m/z $[M]^+$ calculated for $C_{26}H_{10}O_{12}N_6$ 598.03512, found 598.03400.

Synthesis of graphene oxide (GO)

Graphene oxide (GO) was synthesized by the modified Hummers method. The graphite powder (2 g) and $NaNO_3$ (1 g) were well dissolved in concentrated H_2SO_4 (50 mL), and the mixture was stirred vigorously for 30 min in an ice bath. $KMnO_4$ (6 g) was added very slowly into the dark suspension, and the reaction mixture was stirred for another 30 min under a reaction temperature of 20 °C. Then, the ice bath was removed, and the mixture was stirred at room temperature overnight. Distilled water (100 mL) was added to the pasty solution under magnetic stirring, and the solution's color turned yellowish brown. After another 2 h of vigorous stirring, H_2O_2 (30 wt.%, 20 mL) was added dropwise, and the color turned golden yellow immediately. The mixture was washed with 5% HCl several times and then with deionized water until the solution became neutral. The reaction mixture was filtered and dried in a vacuum oven at 40 °C for 12 h. The GO was obtained as a gray powder and used for further experiments. The synthesis of rGO is as per our previous report.[S2]

NOTE S2

The following formula calculates the average potential:

$$V_{av.} = \frac{\int_0^{Q_T} V dq}{Q_T} \quad \textbf{(1)}$$

Here, "V_{av}" is the average voltage, "Q_T" is the total cycle capacity, and the integral is the area under the discharge curve.

The Galvanostatic Intermittent Titration Technique (GITT) was used to quantify the ions' diffusion coefficients, estimated using equation (1), shown below.

The formula for determining GITT using *Fick's second law*:

$$D = \frac{4L^2}{\pi\tau}\left(\frac{\Delta E_s}{\Delta E_\tau}\right)^2 \quad \textbf{(2)}$$

Here, L is the ion diffusion distance (cm), and the pulse time of the current pulse is denoted by τ (s). "ΔE_s" is the voltage difference measured at the end of the relaxation period for two successive steps, and "ΔE_τ" is the difference between the initial voltage and final voltage during the discharge pulse time after eliminating the IR drop.

NOTE S3

The reduction and oxidation reactions of NDI-2NO_2 and NDI-4NO_2 involve lithium ions' electrochemical insertion and deinsertion, as shown in below Figure (a and b). During the discharge process, the NDI molecules undergo reduction, and the carbonyl groups within them can coordinate with lithium ions to form lithium enolates. This insertion occurs in two steps, where two lithium ions are sequentially inserted into the NDI molecule. Conversely, during the charging process, the lithium ions are deinserted from the NDI molecule in a reverse fashion.[S3]

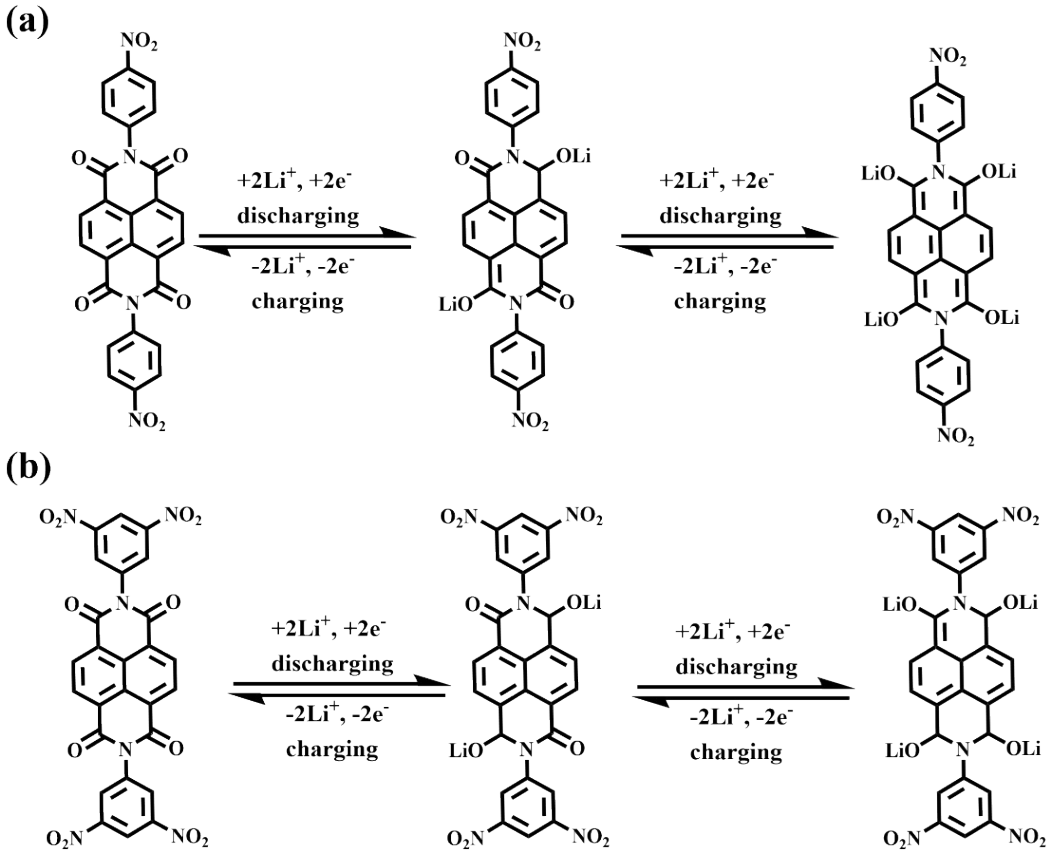

Plausible redox mechanism of (a) NDI-2NO_2 and (b) NDI-4NO_2.

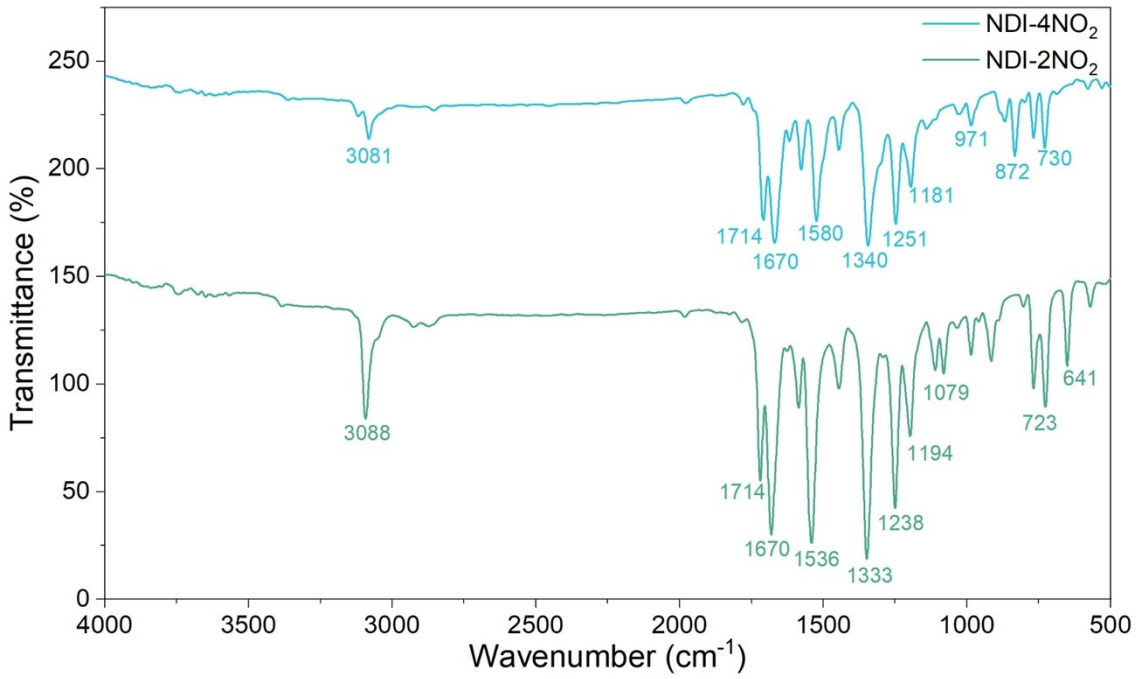

Figure S1. Comparative FT-IR spectra of NDI-2NO_2 and NDI-4NO_2 molecules.

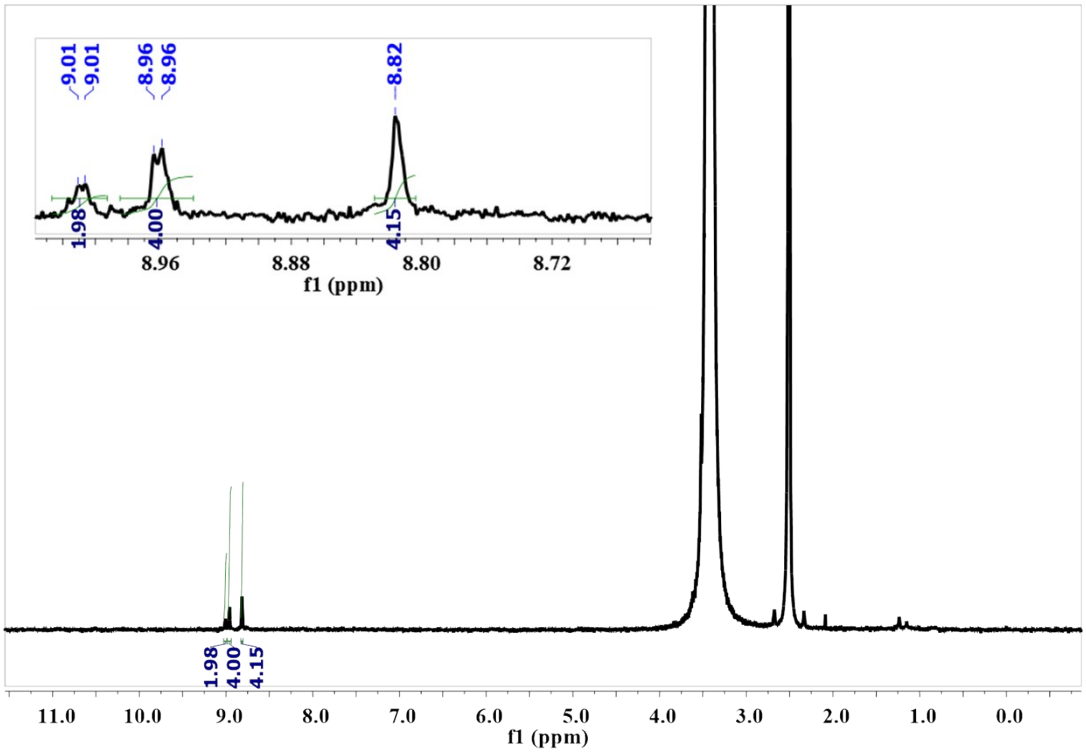

Figure S2. Nuclear Magnetic Resonance (^{1}H-NMR) spectroscopy of NDI-4NO_2.

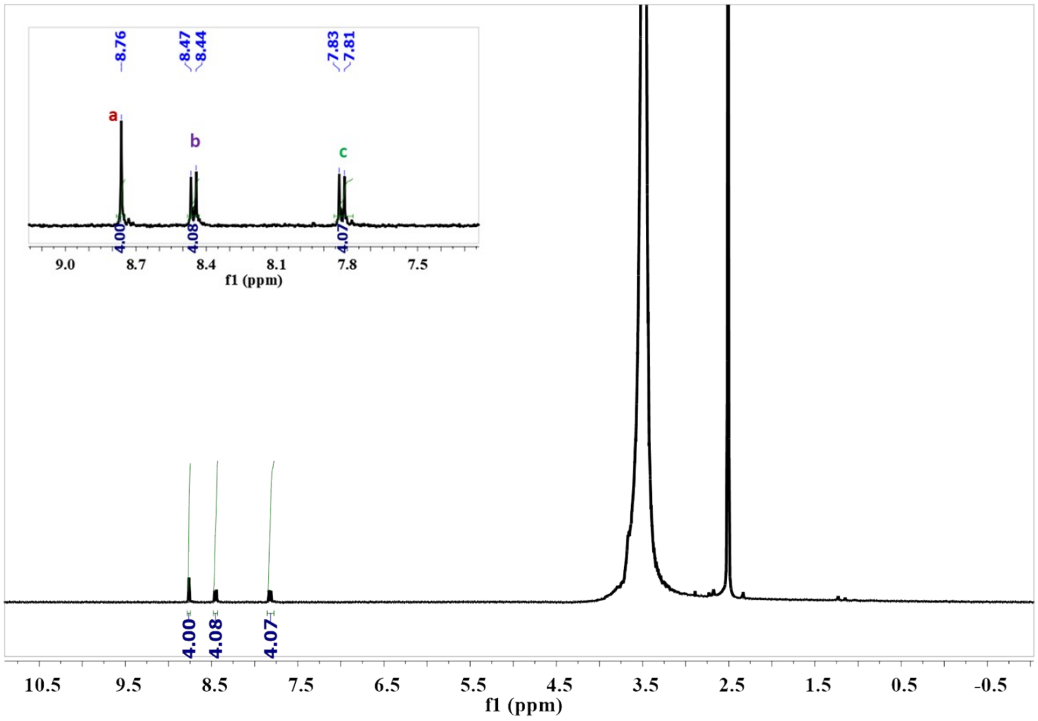

Figure S3. ^{1}H-NMR of NDI-2NO_2.

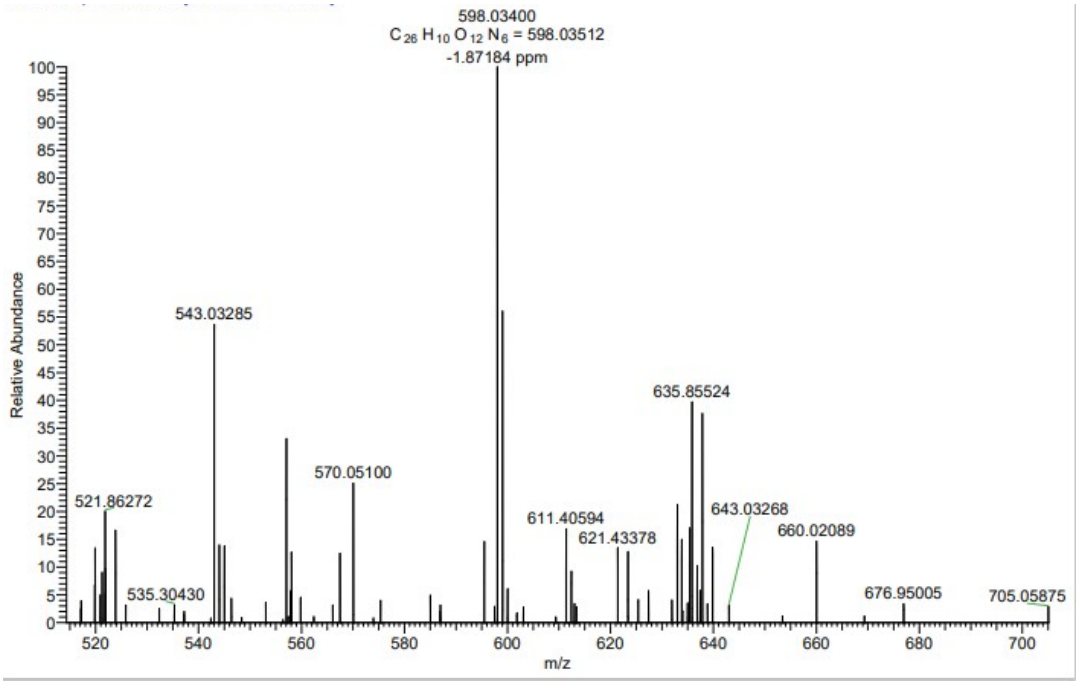

Figure S4. High-Resolution Mass Spectroscopy (HRMS) of NDI-4NO_2

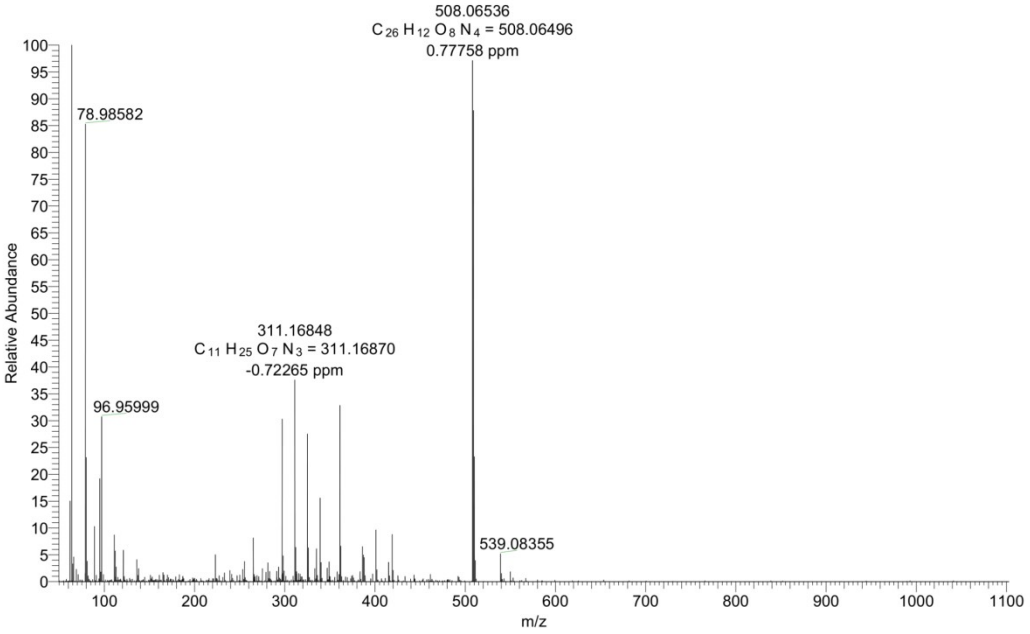

Figure S5. HRMS of NDI-2NO_2.

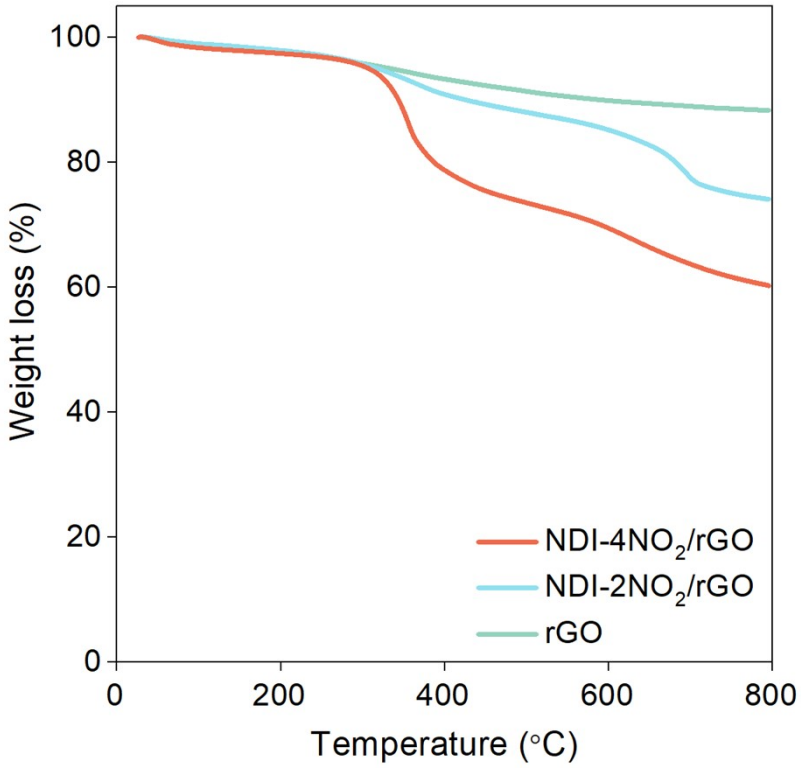

Figure S6. TGA analysis for NDI-4NO_2/rGO, NDI-2NO_2/rGO and rGO samples.

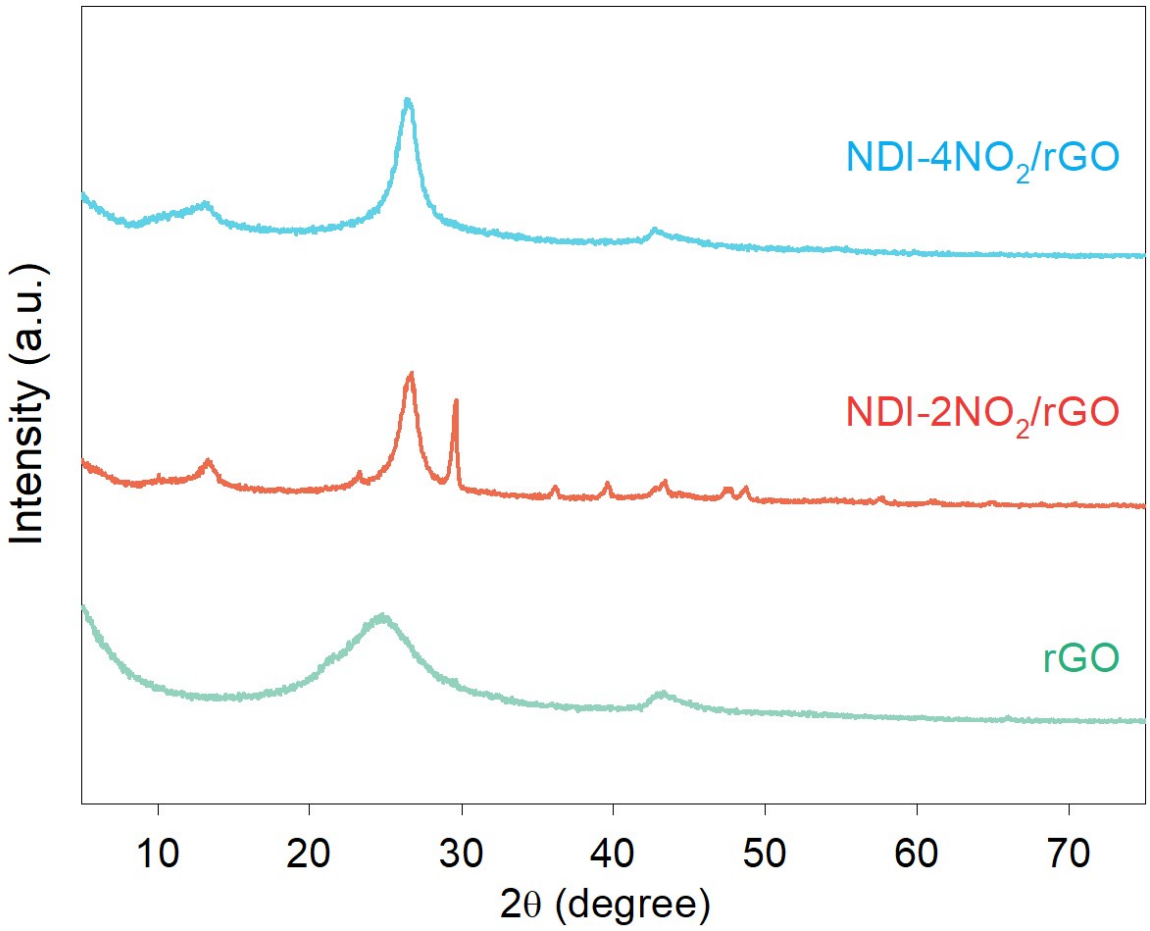

Figure S7. PXRD spectra for rGO, NDI-$4NO_2$/rGO, and NDI-$2NO_2$/rGO.

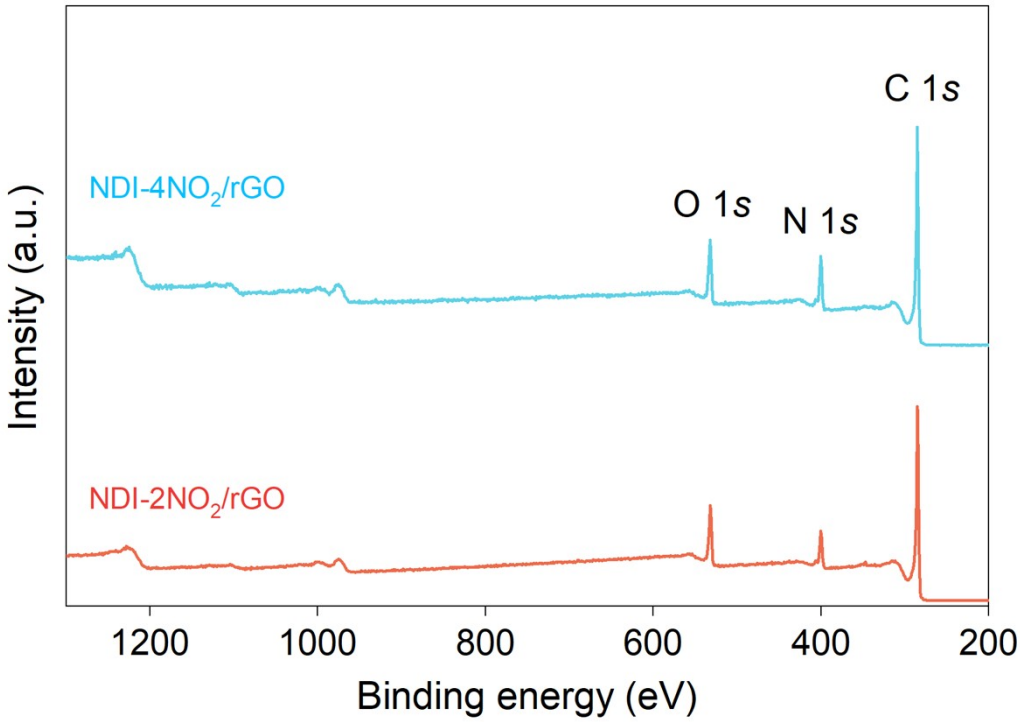

Figure S8. Comparative XPS spectra of NDI-4NO_2/rGO and NDI-2NO_2/rGO samples.

Table S1. Atomic % distribution of elements and corresponding bonding present in the NDI-4NO_2/rGO sample.

Element	Atomic %
C 1s	72.95
N 1s	13.89
O 1s	13.15

Table S2. Atomic % distribution of elements and corresponding bonding present in the NDI-2NO_2/rGO sample.

Name	Atomic %
C 1s	75.94
N 1s	10.83
O 1s	13.21

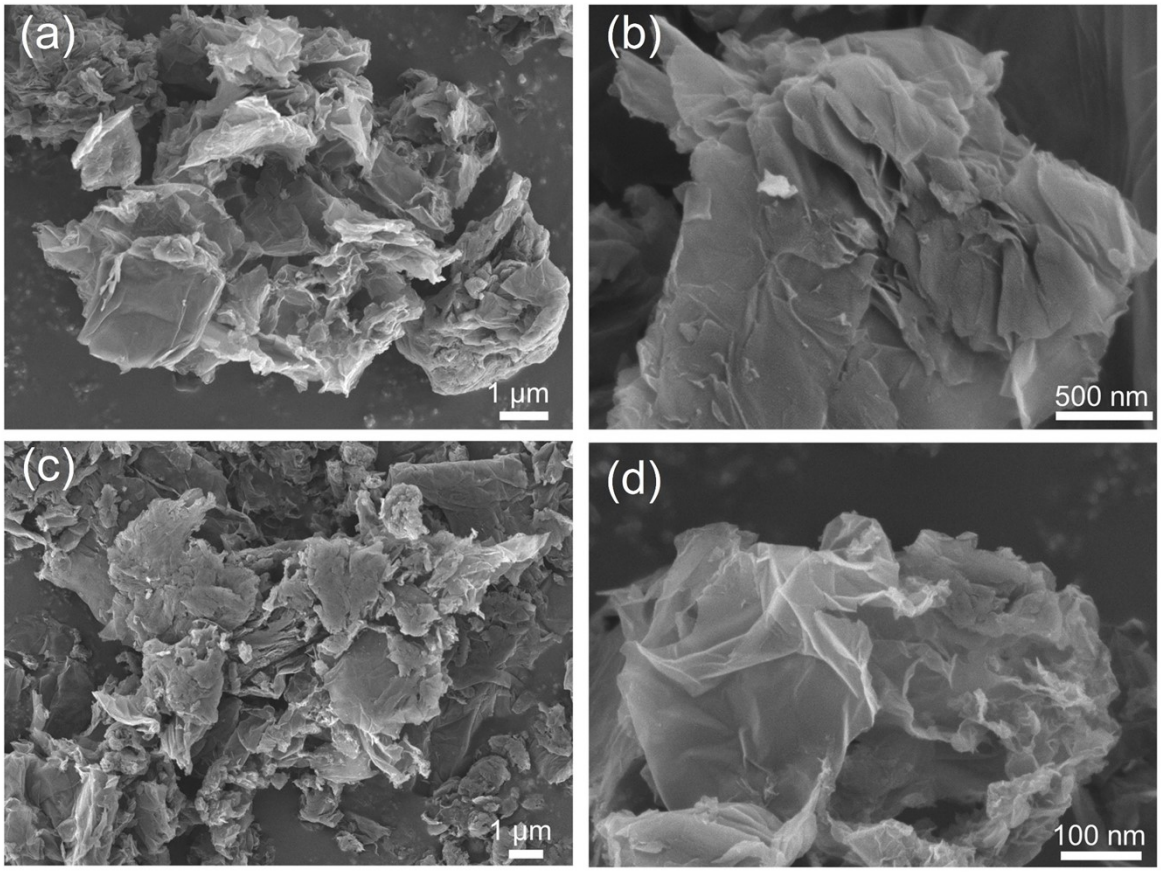

Figure S9. FESEM images of NDI-4NO_2/rGO and NDI-2NO_2/rGO and composites. FESEM images of NDI-2NO_2/rGO at (a) low and (b) high magnification. FESEM images of NDI-4NO_2/rGO at (c) low and (d) high magnification.

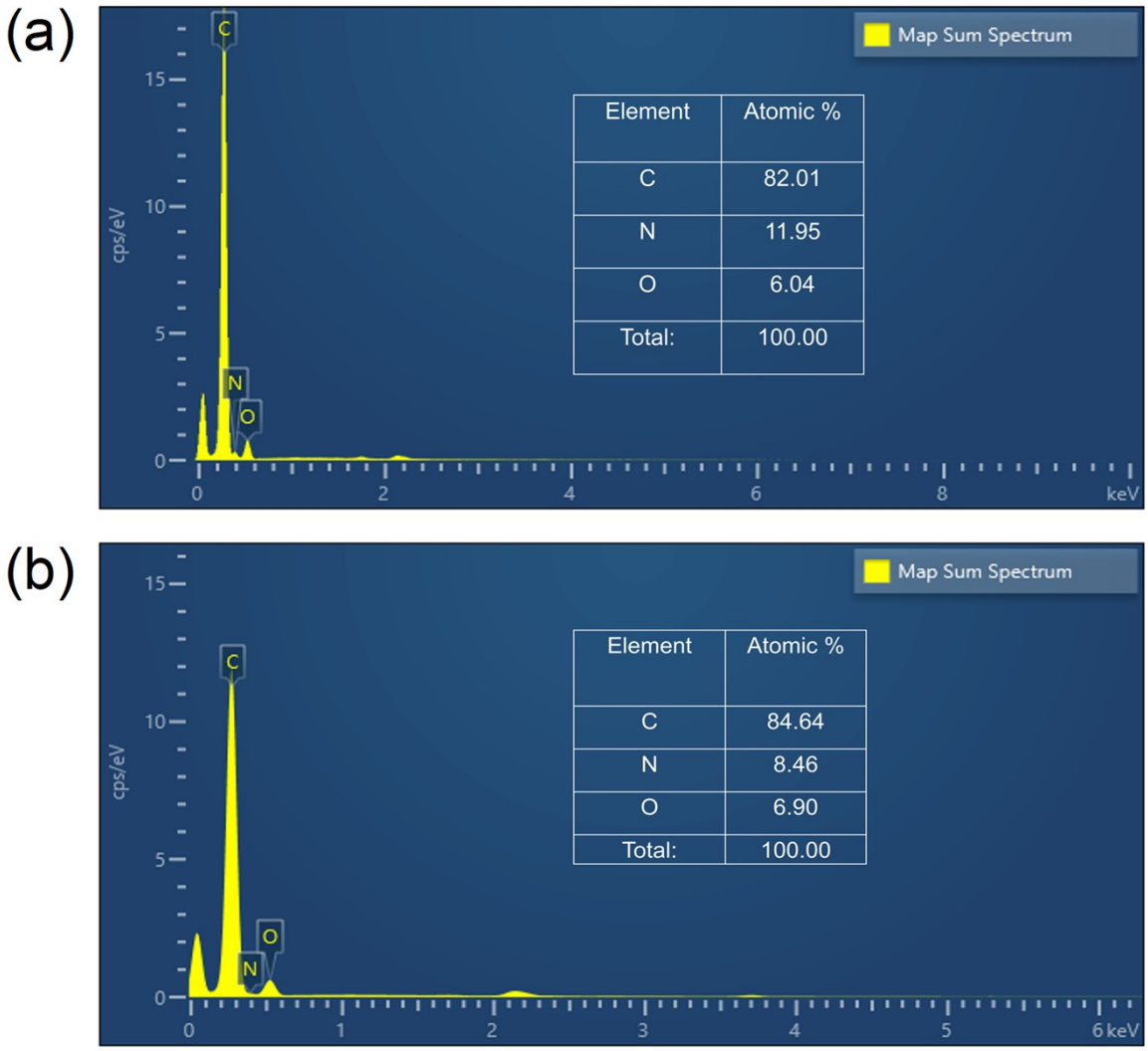

Figure S10. EDS mapping spectra of (a) NDI-4NO_2/rGO, (b)NDI-2NO_2/rGO.

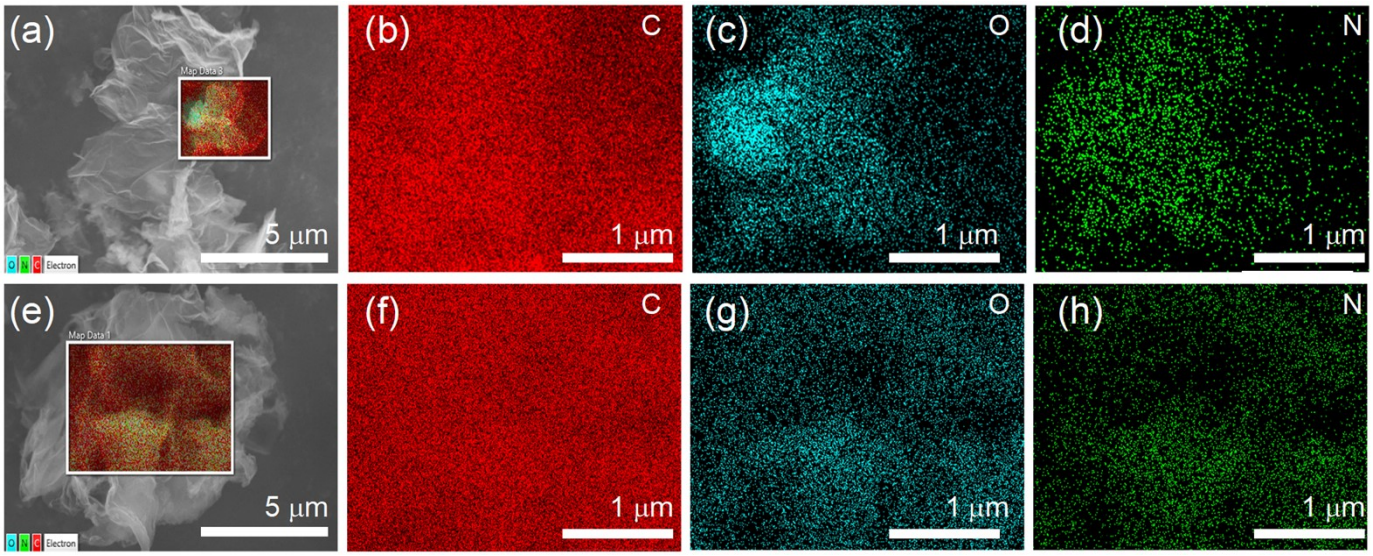

Figure S11. EDS mapping (a) EDS overlapped image of NDI-4NO_2/rGO mapping for different elements, (b) carbon, (c) oxygen and (d) nitrogen. (e) EDS overlapped image of NDI-2NO_2/rGO mapping for different elements (f) carbon, (g) oxygen and (h) nitrogen.

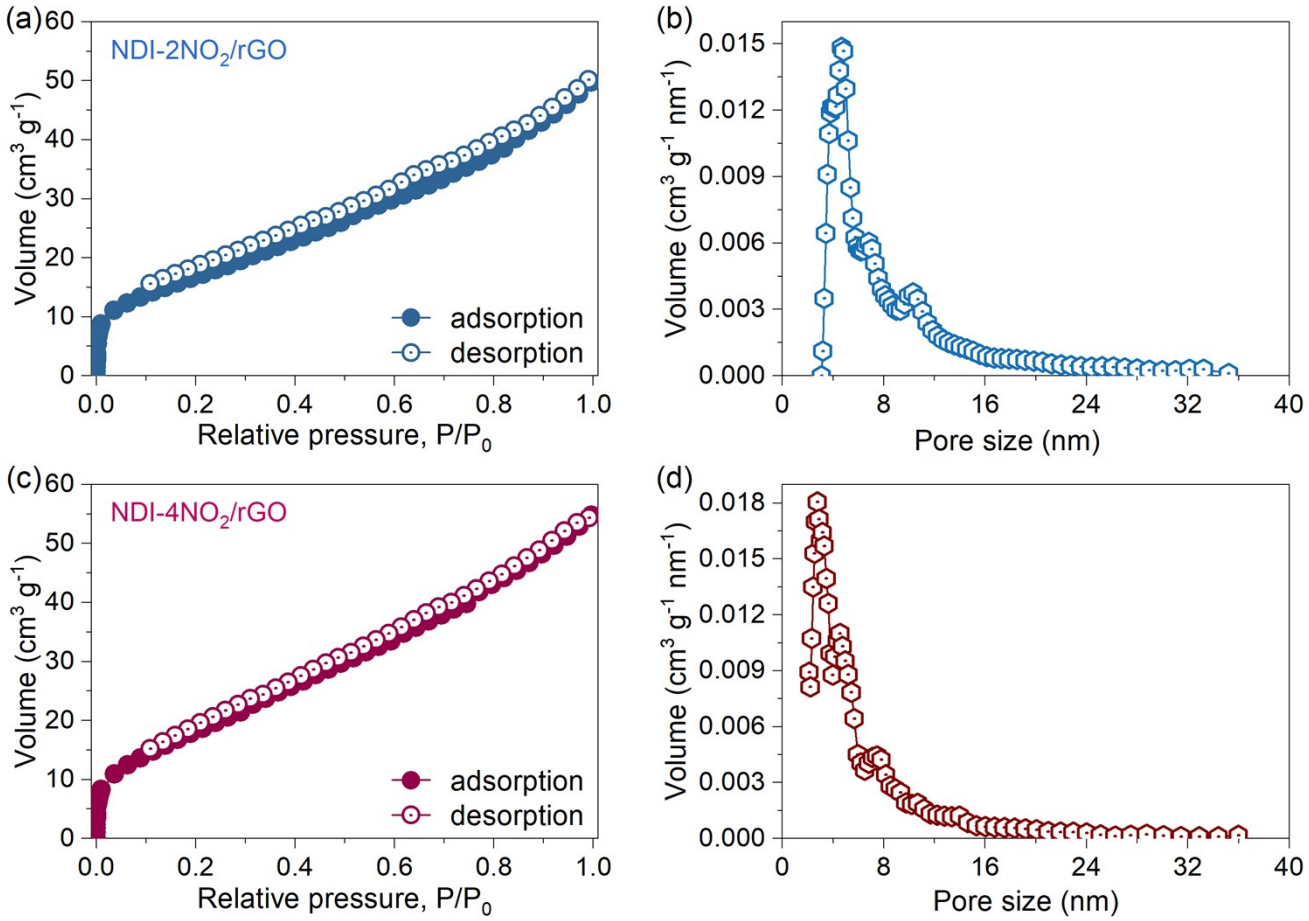

Figure S12. Nitrogen adsorption-desorption isotherm for (a) NDI-4NO_2/rGO and (c) NDI-4NO_2/rGO composites. Pore size distribution of (b) NDI-2NO_2/rGO and (d) NDI-4NO_2/rGO composites.

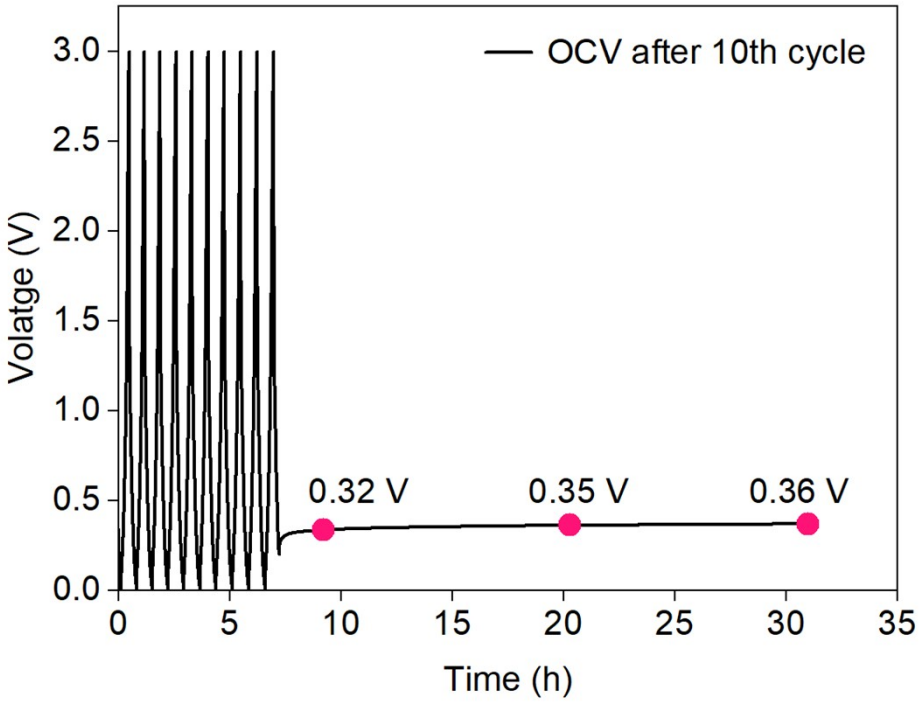

Figure S13. OCV plot of NDI-4NO_2/rGO after 10 charge-discharge cycles.

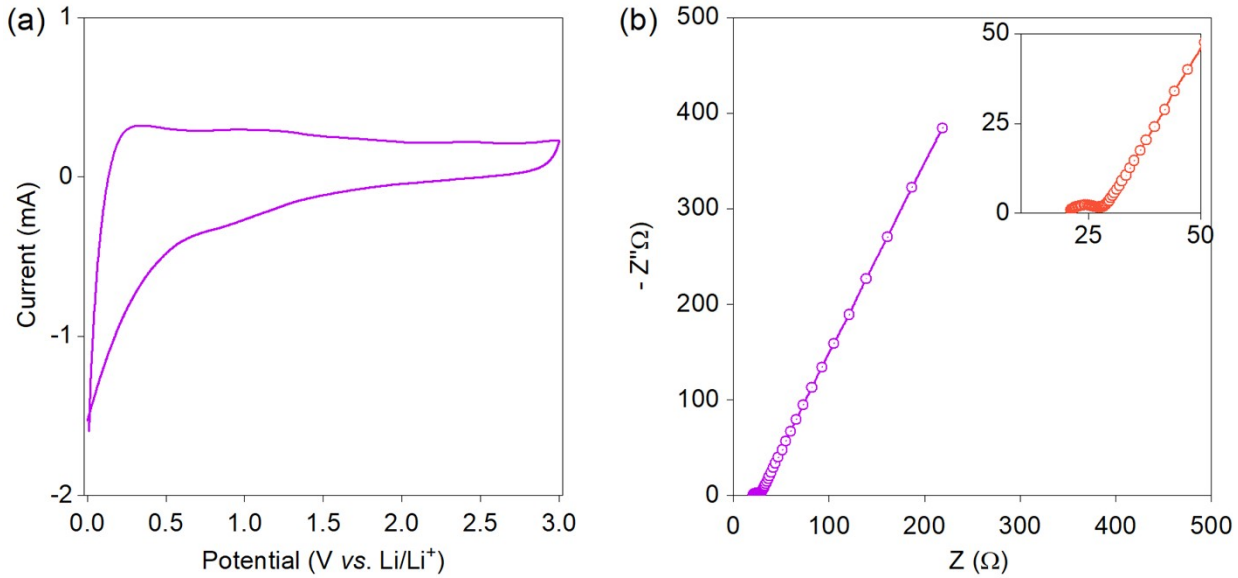

Figure S14. (a) CV plot for the rGO sample, and (b) the Nyquist plot for rGO, inset shows the zoomed-in image for the Nyquist plot.

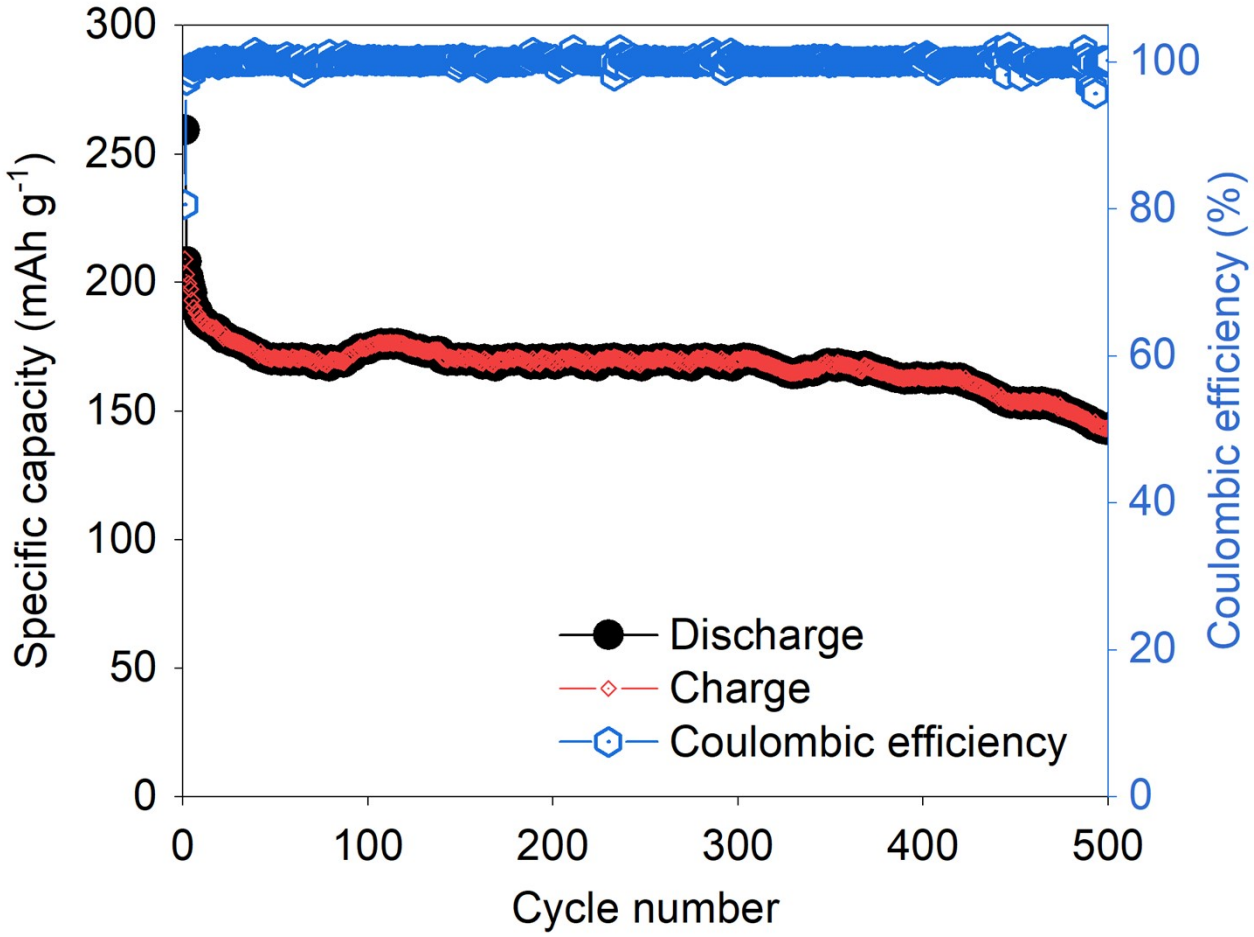

Figure S15. Cycle life test at 1 A g^{-1} for NDI-2NO_2/rGO sample. The half-cell retains about 74% of its initial discharge capacity after 500 cycles.

Table S3. Comparison of our materials with various literature reports for organic material-based electrodes for LIBs applications.

Sample Name	Capacity (mAh g^{-1})	Current density	No. of cycles	Capacity retention (%) @ current density	Ref.
CL-DVP-NDI*	121.3	0.2 C	200	84 @ 1C	S4
G@PI/rGO*	198.0	30 mA g^{-1}	2500	70 @ 1 A g^{-1}	S5
PTCDA/CNT*	115.0	2 C	300	93 @ 0.1 A g^{-1}	S6
DP-NTCDI-250*	170	25 mA g^{-1}	100	70 @ 0.025 A g^{-1}	S7
NDIDA-GO*	240	50 mA g^{-1}	50	100 @ 0.050 A g^{-1}	S8
BBL*	317.0	6 C	1000	100 @ 3 C	S9
NDI-2NO_2/rGO	560.0	50 mA g^{-1}	500	74@ 1 A g^{-1}	**This work**
NDI-4NO_2/rGO	699.0	50 mA g^{-1}	800	89@ 1 A g^{-1}	

Note:** ***CL-DVP-NDI *= N,N'-Di(4'-vinylphenyl)-naphthalene-1,4,5,8-dicarboxydiimide;* ***G@PI/rGO*** *= graphene@polyimide /reduced graphene oxide;* ***PTCDA/CNT*** *= poly(3,4,9,10-perylenetetracarboxylic dianhydride ethylene diamine)/carbon nanotube;* ***DP-NTCDI-250*** *= N,N'-diphenyl-1,4,5,8-naphthalenetetra-carboxylic diimide;* ***NDIDA-GO*** *= naphthalenediimide diamine-graphene oxide;* ***BBL*** *= poly(benzobisimidazobenzophenanthroline).*

References

S1. S. U. Sharma, Y. L. Chang, S. V. Chaganti, Y. W. More and J. T. Lee, *ACS Appl. Energy Mater.*, 2022, **5**, 7550–7558.

S8. A. B. Deshmukh, M. R. Biradar, M. D. Pawar, S. V. Bhosale and M. V. Shelke, *J. Energy Storage*, 2022, **56**, 106036.

S9. Z. P. Song, H. Zhan and Y. H. Zhou, *Angew. Chem. Int. Ed.*, 2010, **49**, 8444–8448.

S4. Sharma, S. U.; Chang, Y. L.; Chaganti, S. V.; More, Y. W.; Lee, J. T. Cross-Linked Naphthalene Diimide-Based Polymer as a Cathode Material for High-Performance Organic Batteries. *Appl. Energy Mater.* 2022, **5**, 7550–7558.

S5. Chang, B.; Ma, J.; Jiang, T.; Gao, L.; Li, Y.; Zhou, M.; Huang, Y.; Han, S. Reduced Graphene Oxide Promoted Assembly of Graphene@polyimide Film as a Flexible Cathode for High-performance Lithium-ion Battery, *RSC Adv.*, 2020,**10**, 8729-8734.

S6. Wu, H.; Wang, K.; Meng, Y.; Lu, K.; Wei, Z. An Organic Cathode Material Based on a Polyimide/CNT Nanocomposite for Lithium-ion Batteries, *J. Mater. Chem. A*, 2013, **1**, 6366-6372.

S7. Lv, M.; Zhang, F.; Wu, Y.; Chen, M.; Yao, C.; Nan, J.; Shu, D.; Zeng, R.; Zeng, H.; Chou, S. L. Heteroaromatic Organic Compound with Conjugated Multi-carbonyl as Cathode Material for Rechargeable Lithium Batteries. *Sci. Rep.*, 2016, **6**, 23515.

S8. Song, Y.; Gao, Y.; Rong, H.; Wen, H.; Sha, Y.; Zhang, H.; Liu, H. J.; Liu, Q. Functionalization of Graphene oxide with Naphthalenediimide Diamine for High-performance Cathode Materials of Lithium-ion Batteries, *Sustainable Energy Fuels*, 2018, **2**, 803-810.

S9. Wu, J.; Rui, X.; Wang, C.; Pei, W. B.; Lau, R.; Yan, Q.; Zhang, Q. Nanostructured Conjugated Ladder Polymers for Stable and Fast Lithium Storage Anodes with High-Capacity, *Adv. Energy Mater.* 2015, **5**, 1402189.